Journal of Radioanalytical and Nuclear Chemistry (2019) 322:147–155
https://doi.org/10.1007/s10967-019-06632-4

Characterization of dry tube location in KAMINI reactor towards the development of k_0-based IM-NAA

Manish Chand[1,2] · **J. S. Brahmaji Rao**[2] · **G. V. S. Ashok Kumar**[2] · **R. Kumar**[1,2]

Received: 13 February 2019 / Published online: 5 July 2019

Abstract

Characterization studies were carried out for the freshly installed dry tubes (DT-1 and DT-2) in KAMINI reactor. The maximum gold equivalent neutron flux at 20 kW for DT-1 and DT-2 were found to be (1.02 ± 0.02)E+10 cm^{-2} s^{-1} at 368 and (4.90 ± 0.30)E+7 cm^{-2} s^{-1} at 300 mm respectively. The sub-cadmium to epithermal neutron flux ratio (*f*) and epithermal neutron flux shape factor (α) were found to be 144 ± 7 and − 0.289 ± 0.010 respectively at this position for DT-1 alone. These parameters were validated by analyzing the IAEA standard (SL-1) and applied to analyze jarosite samples using k_0-based internal monostandard neutron activation analysis.

Keywords KAMINI reactor · Sub-cadmium to epithermal neutron flux ratio · Epithermal neutron flux shape factor · IM-NAA · In-situ relative detection efficiency

Introduction

Elemental analysis of small to large samples [1–4] with irregular geometry is always a challenging task in comparison with the conventional samples and often questionable in terms of true analytical representativeness. Routine analysis of such samples demands sub-sampling and other laborious sampling methodologies. Samples which are precious in nature or difficult to dissolve or with irregular size and shape require special analytical methods. Development of non-destructive analytical techniques is preferable for both analytical as well as economical reasons [4–7] for the above referred samples. NAA is one of the non-destructive analytical techniques used to establish the elemental profile of samples in a wide varieties of matrices.

There are several standardization methods such as absolute, relative and k_0-method [8] that exist in NAA with their associated merits and limitations. The most frequently used method is the relative NAA, which demands a priori knowledge of the analytes present in the sample to be analyzed. This necessitates either individual elemental standards or suitable multi-elemental standards like certified reference materials (CRMs) that are to be irradiated simultaneously along with the sample towards the estimation of its elemental composition. Sometimes, CRMs may not have included our element of interest and also irradiating multi standards may encounter some practical difficulties. In such cases, use of a single comparator like gold (Au) instead of multi standards is preferable for assaying the spectrum of elements present in the samples, which is known as k_0-NAA method [9–12]. In this case, the knowledge of a composite nuclear constant (k_0), absolute efficiency of the detector and parameters based on the irradiation position in a reactor such as sub-cadmium to epithermal neutron flux ratio (*f*) and epithermal neutron flux shape factor (α) are required. However, the major challenge involved in this method for the analysis of large or irregular samples is to address the challenges maintaining the consistency of the efficiency which is otherwise disturbed by [13] (1) The variation of neutron flux across the sample during the irradiation (2) The self-attenuation of gamma rays within the sample volume and (3) The practical limitations in preparing standard with identical geometry of the sample.

A k_0-based internal monostandard neutron activation analysis (IM-NAA) method [5, 6] for non-destructive analysis of elements in irregular samples is an attractive option for many applications such as the analysis of

---

✉ R. Kumar
rkumar@igcar.gov.in

[1] Homi Bhabha National Institute (HBNI), Indira Gandhi Centre for Atomic Research, Kalpakkam 603102, India

[2] Fuel Chemistry Division, Indira Gandhi Centre for Atomic Research, Kalpakkam 603102, India

precious archaeological, geological, biological, environmental, alloy and special nuclear samples [7, 14]. This is an efficient method, developed by Nair et al. [6, 15] in 2003 for the analysis of large and non-standard geometry samples and provides relative concentration of an element with respect to the monostandard that is present within the sample itself. The absolute elemental concentration can be obtained from these ratios for the samples such as metals and alloys by using the mass balance, if all the major and minor elements are established by NAA. Otherwise, knowledge on the concentration of the monostandard or any other element in the sample is needed to establish the absolute concentrations of the other elements. The neutron flux perturbation within the sample, if any, during the irradiation would be mitigated by considering the internal monostandard. Further, gamma rays from various activated products of each sample would be used to obtain the in situ relative detection efficiency [14–16] that would also mitigate the perturbation in the detection efficiency due to γ-ray self-attenuation and geometrical effects of the sample. The above mentioned advantages make IM-NAA as a unique and geometry independent method and thus enhancing the applicability of the k_0-NAA method. The concentration ratio of an element (x) with respect to the internal monostandard (y) in k_0-based IM-NAA is calculated using the following Eq. (1)

$$\frac{m_x}{m_y} = \frac{\left((SDC)\left(f + Q_0(\alpha)\right)\right)_y}{\left((SDC)\left(f + Q_0(\alpha)\right)\right)_x} \cdot \frac{PA_x}{PA_y} \cdot \frac{\left(\varepsilon_\gamma\right)_y}{\left(\varepsilon_\gamma\right)_x} \cdot \frac{k_{0,\mathrm{Au}}(y)}{k_{0,\mathrm{Au}}(x)} \quad (1)$$

where S is the saturation factor, D is the decay correction factor, C is the counting correction factor, $Q_0(\alpha)$ is the ratio of the resonance integral (I_0) to thermal neutron cross section (σ_0) corrected for α, PA is the net peak area of the interested gamma lines from the same spectrum, $k_{0,\mathrm{Au}}$ is the literature reported $k_{0,\mathrm{Au}}$-factors [12] and ε_γ is the in situ detection efficiency [16].

The reliability of the method depends on the accurate knowledge of the reactor based parameters f and α as they vary with the irradiation position in the nuclear reactor [17]. The f value determines the thermal and epithermal flux components present at the irradiation locations, whereas, α represents the shape of the non-ideal epithermal neutron spectrum. In an ideal case, neutron flux spectrum in epithermal region follows 1/E law, but in practical cases, it invariably deviates from the ideality and rather follows $1/E^{1+\alpha}$ [18–22]. The α value can be either positive or negative depending upon the irradiation position with respect to the reactor core, which may indicate ‘‘softened’’ or ‘hardened’’ epithermal neutron spectrum, respectively. The α value is used to calculate the $Q_0(\alpha)$ [18–22].

KAMINI reactor: a neutron source for NAA

KAMINI (KAlpakkam MINI) is a unique research reactor (30 kW power) which is operational at Indira Gandhi Centre for Atomic Research, Kalpakkam with ^{233}U as the fuel. The fuel is in the form of plates of an alloy of ^{233}U and aluminium which are assembled in an aluminium casing to constitute the fuel subassembly. The reactor has three beam tubes, two thimble irradiation locations and one pneumatic fast transfer system (PFTS) (Fig. 1), which are used to carryout irradiation experiments towards radiography, shielding experiments, activation analysis, radiation physics research and testing of neutron detectors.

Recently, two dry tubes were installed in the KAMINI reactor, namely DT-1 and DT-2. These dry tubes are made up of aluminium and positioned just outside the BeO reflector blocks in the west and south side of the reactor as shown in Fig. 1. These dry tubes are installed for the neutron activation analysis studies and for testing the neutron detectors developed by Bhabha Atomic Research Centre (BARC), Mumbai as well as Electronics Corporation of India Limited (ECIL), Hyderabad. The DT-1 is positioned at a distance of 350 mm from the centre of the reactor core and placed on the base plate with the height, inner and outer diameter of the tube being 3750, 75 and 80 mm respectively. Similarly, the DT-2 is positioned on ring collar at a distance of 900 mm away from the centre of the reactor core with height, inner and outer diameter of the tube being 3750, 103 and 109 mm respectively. These dry tubes are sufficiently large and characterization of these positions towards the determination of neutron flux, f and α is a mandatory requirement to carryout the k_0-based IM-NAA experiments.

Characterization of the various irradiation positions i.e. PFTS, thimble location and beam tubes were already accomplished and reported elsewhere i.e. Ashok et al. [23] characterized the PFTS position and Mohapatra et al. [24, 25] characterized thimble and beam tube locations of KAMINI reactor. Brahmaji Rao et al. [17] validated k_0-NAA method at PFTS position for the reference materials (1) NIST SRM 1646a (Estuarine Sediment) and (2) BCS Nb-stabilized Stainless Steel (BCS/SS No.261/1). Swain et al. [26] analyzed Synthetic MultiELement Standards (SMELS) by k_0-based IM-NAA using PFTS of KAMINI reactor for an exercise towards its quality control and reported relative concentration ratios of 22 elements with respect to gold as the internal monostandard.

The present work established the neutron flux profiles inside the dry tubes i.e. DT-1 and DT-2 and the flux determination was carried out from the bottom of the tubes. However, the characterization towards the determination of f and α has been carried out for DT-1 only initially.

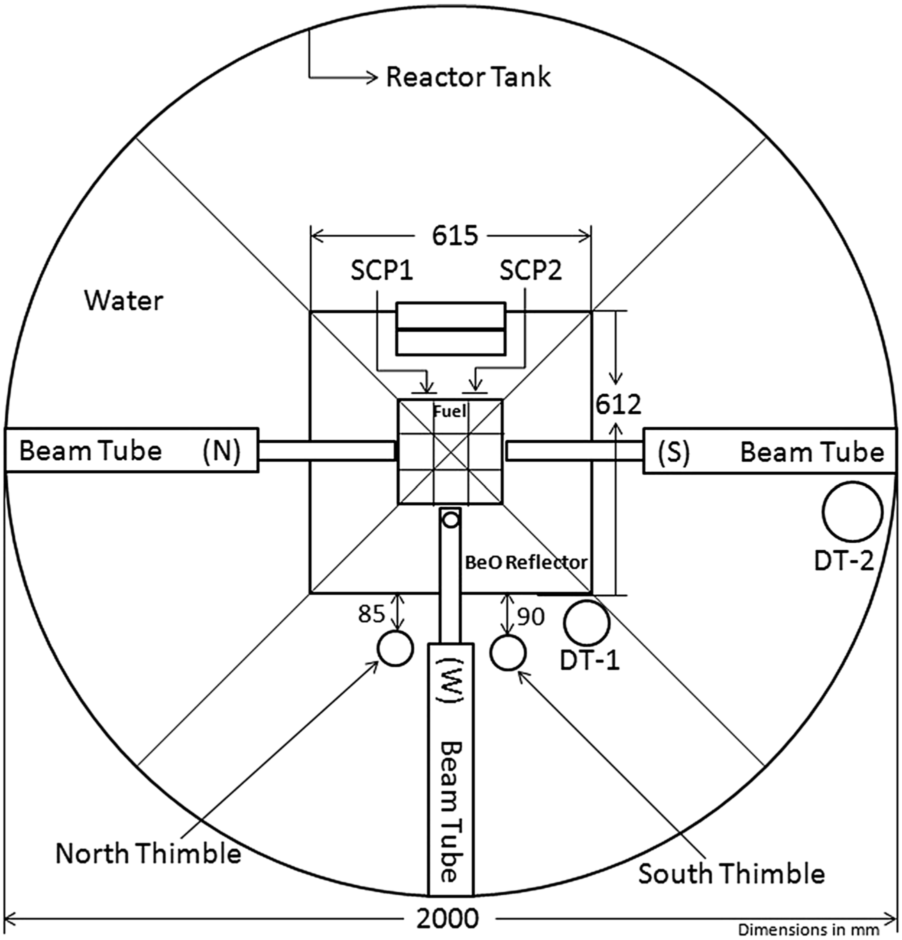

Fig. 1 Horizontal cross-sectional view of the KAMINI reactor with irradiation sites. (The unit for the numbers mentioned in the above picture is mm and DT-1 and 2 represent dry tube-1 and 2 respectively)

The α values were measured using cadmium-ratio and cover methods, whereas, the f values were measured using cadmium-ratio method. The f and α values so obtained in DT-1 were validated using CRM IAEA Lake Sediment (SL-1) by k_0-based IM-NAA.

Jarosites are produced in high quantities as solid residues during the extraction of zinc from zinc sulphide ores. About 13 Mt of zinc is produced annually worldwide and India is the second largest and also one of the cheapest Zinc–Lead producers [27]. Hindustan Zinc Limited (HZL) is India's only integrated Zinc–Lead–Silver producer located in the states of Rajasthan, Andhra Pradesh, Bihar and Odisha as a multi-unit mining and smelting organization with a capacity of 3.5 Mt of Zinc per year. In India, about 0.25 Mt of jarosite per annum is being produced [28]. The jarosite mainly constitutes of toxic elements like chromium, cadmium, arsenic, lead, aluminium etc. Due to their toxic nature, disposal and storage of these jarosite residues without further treatment becomes a major environmental and ecological concern. The disposal and the subsequent impact on the environment with the evaluation of its recycling (or) utilization potential demand the characterization of the jarosite waste with its corresponding elemental composition [29]. However, conventional analytical techniques would generally demand the destruction of the sample followed by separation of specific analytes of interest, for the estimation of its elemental composition. The validity of the method demands further a quantitative dissolution of the sample besides demanding a cumbersome separation procedure. Non-destructive assay using NAA is an attractive alternate analytical tool for the determination of elemental composition of such samples. The k_0-based IM-NAA method was subsequently applied to two jarosite samples received from National Metallurgical Laboratory, Council of Scientific and Industrial Research (CSIR), Jamshedpur, India to obtain their elemental profile and reported using IM-NAA method.

Experimental

Materials and equipment

The activation foils such as Au and Zr of purity > 99.9% used in this study were procured from Good-fellow foils, U.K. The assay of the irradiated activation foils was accomplished by high resolution gamma spectrometry using a 30%

co-axial High Purity Germanium (HPGe) detector procured from M/s Eurisys Mesures. The detector has a resolution of 1.85 keV at 1332 keV of ^{60}Co and coupled with an associated PC based 8 k multichannel analyzer (MCA) ISA card of Aptec along with acquisition software. Energy calibration of the detector was established using the standard sources of ^{241}Am, ^{137}Cs, ^{133}Ba and ^{152}Eu, which were procured from M/s Amersham, Inc.

Characterization of dry tube

Axial flux profile

Typically the flux along the axial direction of DT-1 was monitored by irradiating multiple standard sources of gold solution. These standard sources secured at predetermined heights using a thread hanging axially along the tube from the top that extended up to the bottom of the tube covering a total height of a meter. However, the gold standard sources fastened at the bottom of the thread was only accommodated in a polypropylene (PP) container of 100 mL capacity, the weight of which was expected to stabilize the hanging position of the thread as well as to ensure the container just touching the bottom position to maintain the height of the source as accurately as possible (Fig. 2). The size of the PP container was chosen based on the inner diameter of the tube such that it can facilitate the irradiation of different sizes of samples. Typically, the gold standard source was prepared by taking a known amount of Au standard solution on a filter paper on weight basis, dried under the IR lamp and doubly sealed. The first Au standard in the PP container was positioned at 37 mm of height from the bottom of DT-1. The height measurement refers to the height from the bottom of the tube. A total of 17 Au flux monitors with the amounts ranging from 100 to 250 µg were fixed axially to the thread inside the DT-1. The flux monitors were all irradiated simultaneously for a period of 2 h at 20 kW power. Experiments with similar design philosophy were carried out to obtain the neutron flux profile inside the DT-2 also.

Determination of *f* and *α*

The activation foils such as Au and Zr with and without cadmium cover of 1 mm thickness and width to length ratio of 1:2 were irradiated for 6 h and 2 h respectively. The Au and Zr foils were positioned at a height of 37 mm which is the centre of the PP container and 368 mm which is the position of maximum flux from the bottom which are the positions expected to be used for NAA. All the irradiated foils were assayed by HPGe detector at a distance of 20 cm and the spectra were analyzed for the peak areas using PHAST peak fitting software.

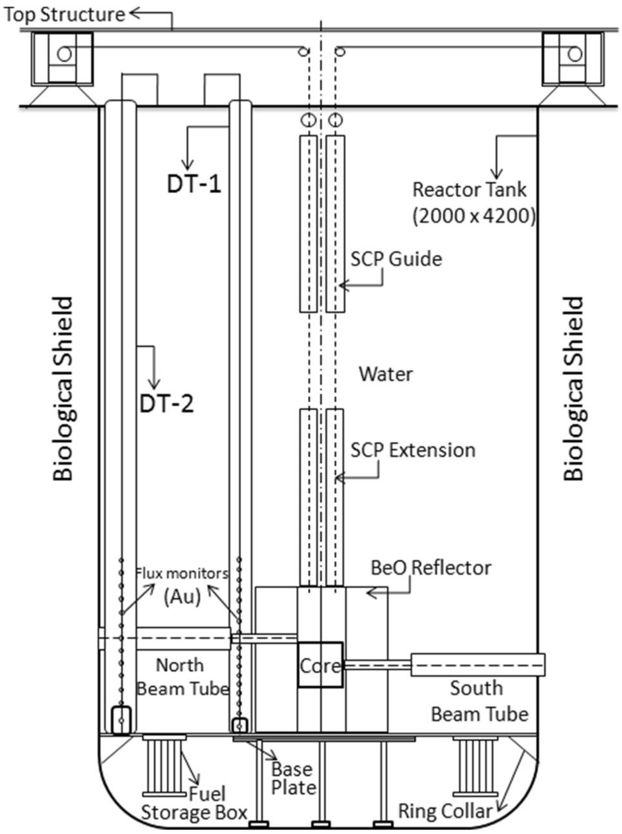

Fig. 2 Irradiation of flux monitors (Au) in dry tubes of KAMINI reactor

Validation of *f* and *α* and their application towards the sample analysis

To validate the freshly characterized reactor parameters of *f* and *α* at the maximum flux position of 368 mm from the bottom of DT-1, an SL-1 standard was analyzed for the elemental concentrations by k_0-based IM-NAA. Approximately 100 mg of the SL-1 was doubly sealed in a polythene cover and irradiated at the peak flux position of DT-1 for 6 h at 20 kW power.

Similarly, two jarosite samples of 5 g each were irradiated at the same position of DT-1 for 6 h at 20 kW power. The packaging materials were also irradiated along with SL-1 and jarosite samples for the sake of blank correction. The irradiated SL-1 standard and two jarosite samples were sufficiently cooled to bring down the corresponding radiation dose and their subsequent radiometric assay was carried out using HPGe detector.

Results and discussion

Characterization of dry tube

Axial flux profile

The neutron flux profile was established for DT-1 using the measured activity of the activated product of gold standard i.e. ^{198}Au from the peak reports of the spectra of the irradiated Au targets. The gold equivalent neutron flux i.e. the neutron flux obtained using the thermal neutron capture cross section for the reaction ^{197}Au(n,γ)^{198}Au, at the different positions were calculated using following Eq. (2)

$$\text{Neutron flux } (\phi) = \frac{A}{N\sigma SDC} \tag{2}$$

where A is the activity of the activated product (dps), N is the number of target nuclides and σ is the cross-section for the ^{197}Au(n,γ)^{198}Au nuclear reaction i.e. 98.65E−24 cm^2.

The calculated neutron flux was plotted as a function of the axial distance from the bottom of the tube DT-1 (Fig. 3). From the figure, it was observed that the flux was increasing with the axial height from the bottom of the tube and peaked at a height of 368 mm which is just parallel and located about the nearest point on the thread in the tube to the core centre point and started decreasing from there on. The maximum neutron flux was observed to be (1.02 ± 0.02) E+10 cm^{-2} s^{-1} at 368 mm. Similarly, the neutron flux at different positions starting from the distance of 67 mm to 1000 mm of the DT-2 was also determined. The neutron flux profile of DT-2 (Fig. 4) was found to be similar to DT-1 and the maximum neutron flux was observed to be (4.90 ± 0.30) E+7 cm^{-2} s^{-1} at 300 mm from the bottom of the tube. The maximum neutron flux at DT-1 was three order higher than that of the DT-2 owing to its closer vicinity to the core compared to the DT-2. The present study focuses on the complete flux profile of DT-1 due to the presence of higher neutron flux for IM-NAA studies and further study towards the augmentation of complete flux profile would be extended to DT-2 also in future.

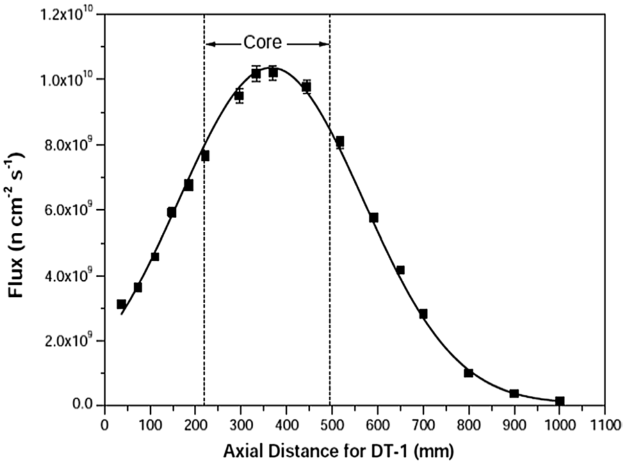

Fig. 3 Variation of neutron flux along the vertical axis of DT-1

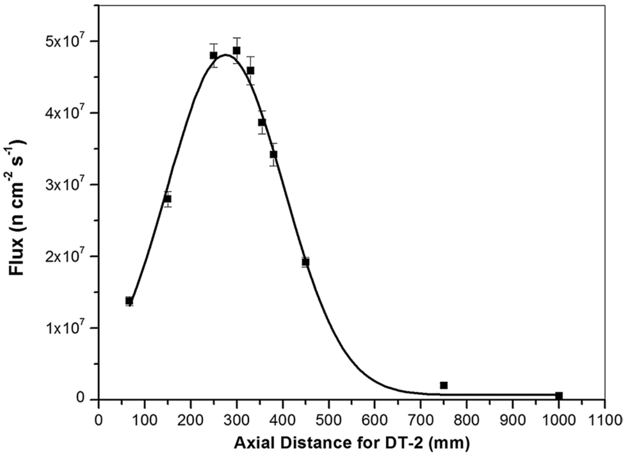

Fig. 4 Variation of neutron flux along the vertical axis of DT-2

Determination of *f* and *α*

The values of f and α were determined using the specific activities of the activated products of the flux monitors Au and Zr i.e. ^{198}Au, ^{95}Zr and ^{97}Zr. In DT-1, the monitors (Au and Zr) were irradiated at two different positions i.e. at 37 and 368 mm from the bottom of the tube. The α values for the DT-1 was estimated by Cd-ratio method using dual monitors as well as Cd-cover triple monitor (^{197}Au, ^{96}Zr, ^{94}Zr) method [20]. The relevant nuclear data of the flux monitors used to determine the f and α are given in Table 1 [12].

In the triple monitor method, the plot of Log(T_i) versus Log($\bar{E}_{r,i}$) was used to obtain the slope ($-\alpha$) as explained in the references [18, 19]. The α value was obtained by iteration procedure [21, 22] using Microsoft Excel sheet. The plot obtained from the final iteration was shown in Fig. 5. The average α value was found to be − 0.273 ± 0.044 at 37 mm and − 0.289 ± 0.010 at 368 mm from the bottom of DT-1. The negative sign of the α values indicates that the neutron spectra at these positions were relatively hard compared to the ideal epithermal neutron flux distribution.

The f values were calculated in the cadmium ratio method [19].

The average f values were found to be 347 ± 18 and 144 ± 7 at 37 mm and 368 mm from the bottom of DT-1 respectively indicating the corresponding presence of 99.7% and 99.3% thermal neutron components respectively. The calculated f and α values are presented in the Table 2. From the table, it can be inferred that the f values increase with

Table 1 The nuclear data of flux monitors

Target	Q_0	Effective resonance energy $\bar{E}_r$ (eV)	Corresponding activated product	$t_{1/2}$	E_γ (keV)	$k_{0,\mathrm{Au}}$ (%uncertainty)
^{197}Au	15.71	5.65	^{198}Au	2.69 d	411.8	1
^{96}Zr	251.6	338	^{97}Zr	16.74 h	743	1.24E−5 (0.3)
^{94}Zr	5.31	6260	^{95}Zr	64.02 d	724.2 756.7	8.90E−5 (1.3) 1.10E−4 (1.3)

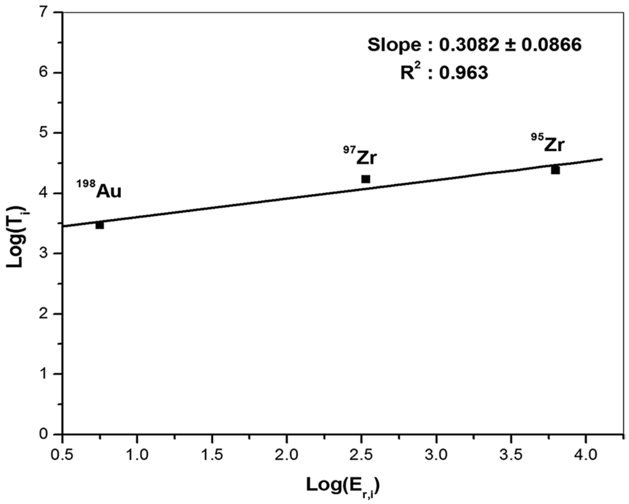

Fig. 5 Log (T_i) versus Log ($\bar{E}_{r,i}$) in Cd-cover method

the decrease in the neutron flux. This may be attributed to the increased moderation of neutrons with distance from the core.

In-situ relative detection efficiency

The activated products of SL-1 and jarosite samples associated with at least one pair of gamma rays with an accurately known intensity and their peak areas were used for the calibration of in situ relative detection efficiency. The activated products of SL-1 i.e. ^{24}Na, ^{56}Mn, ^{140}La and ^{152m}Eu and of jarosite samples i.e. ^{24}Na, ^{46}Sc, ^{59}Fe, ^{124}Sb and ^{140}La were used for the in situ relative efficiency calibration. The whole efficiency curve was obtained by the least square fitting method. The fitted efficiency ratios were obtained using the following Eq. (3) [14–16].

$$\ln(\varepsilon_\gamma) = \sum_{i=0}^{2} A_i \left[\ln(E_\gamma)\right]^i \tag{3}$$

where ε_γ is the in situ detection efficiency and E_γ is the gamma ray energy. A_i's are the coefficients of the second order polynomial. For both SL-1 and jarosite samples, a set of nine such linear equations were iterated for the determination of the coefficients. A typical plot of in situ relative detection efficiency for SL-1 is shown in Fig. 6.

Validation of *f* and *α* and its application towards the sample analysis

The elemental concentration ratio of 11 elements present in the SL-1 were obtained with respect to Sc by k_0-based IM-NAA using the above established values of f and α. The relative concentrations were converted into the absolute concentrations by using certified value of the Sc (Table 3). The comparison of the calculated values with that of the certificate values was accomplished by calculating the % deviation and *Z*-score value. The following Eq. (4) was used to calculate the *Z*-score.

$$Z\text{-score} = \frac{x_i - x_R}{\sigma_R} \tag{4}$$

where x_i is the measured elemental concentration in the present work, x_R is the certified elemental concentration and σ_R is the uncertainty in the elemental concentration of the certificate values of SL-1 at 95% confidence level. The % deviations for the elements determined in SL-1 with respect

Table 2 Results of f and α at DT-1

Characterization parameters		
Distance from the bottom of the dry tube	37 mm	368 mm
Sub-cadmium to epithermal neutron flux ratio (f)	347 ± 18	144 ± 7
Epi-cadmium neutron flux shape factor (α)	− 0.238 ± 0.017^a − 0.308 ± 0.087^b	− 0.289 ± 0.010^a

[a] Cd-ratio method using dual monitors

[b] Cd-cover triple monitor method

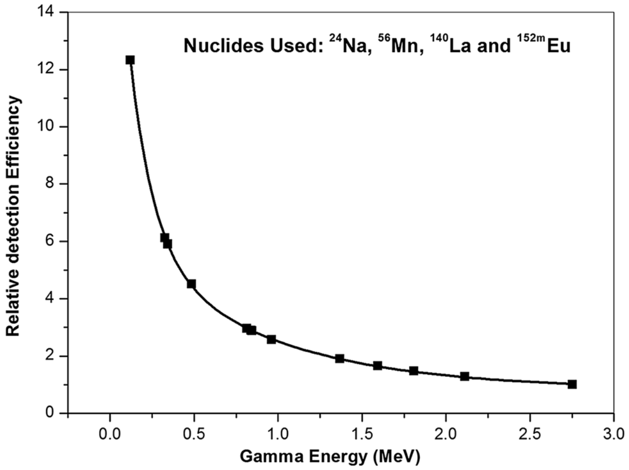

Fig. 6 The variation of in situ relative detection efficiency with the gamma energy for SL-1

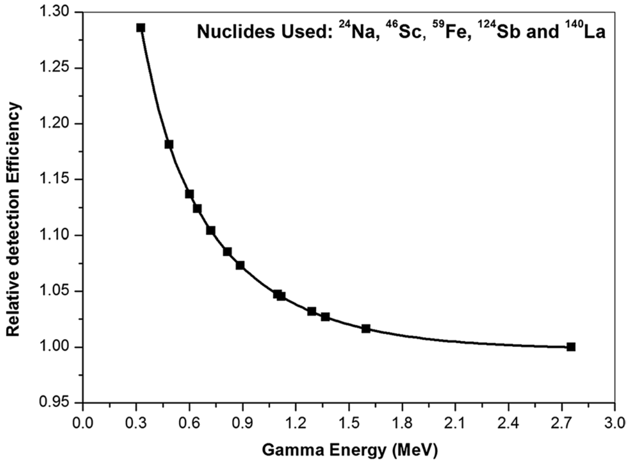

Fig. 7 The variation of in situ relative detection efficiency with the gamma energy for the jarosite sample

to certified values were within ± 5% for most of the elements except for Na (11.8%), Th (8.6%) and As (6.5%) and *Z*-score values at the 95% confidence level were within ± 1 except for Na (2.00), Th (1.20) and Fe (1.18). The accuracy in the elemental concentrations in the SL-1 validates the above characterized irradiation input parameters by using IM-NAA method. The possible interference from the fission product of the Th towards the calculation of the amount of La and Eu in the jarosite samples is negligible owing to the too low fast neutron flux at the irradiation location and Th content in the samples.

The relative elemental concentration of 14 elements present in the jarosite samples were obtained with respect to Sc using in situ relative detection efficiency calibration of the sample as shown in Fig. 7. The relative concentrations were converted into their absolute concentrations by using the concentration of Sc in the same samples obtained by the relative NAA method (Table 4).

The elemental concentrations in jarosite samples vary from ppm to percentage levels. The major elements were found to be iron (15 and 26%), zinc (2.9 and 4.8%) and Na (1 and 2.2%) as shown in the Fig. 8 whereas, the toxic and heavy elements such as arsenic, cadmium, antimony, copper, silver, tungsten etc. were present in trace to minor levels varying from 4 ppm to 0.4%. The presence of these toxic elements makes these jarosites hazardous thus demanding an appropriate disposal protocol.

Table 3 Measured elemental concentration in SL-1 by k_0-based IM-NAA method

Element	Relative conc. wrt Sc	Measured concentration (μg/g)	Certified concentration (μg/g)	% Deviation	*Z* score
La	3.2	55.0 ± 3.8	52.6 ± 3.1	4.6	0.77
Na	108	1900 ± 150	1700 ± 100	11.8	2.00
Mn	205	3600 ± 170	3500 ± 160	2.9	0.63
K	818	14,000 ± 1300	15,000 ± 2100	− 6.7	− 0.48
As	1.7	29.4 ± 1.8	27.6 ± 2.9	6.5	0.62
Eu	0.09	1.56 ± 0.12	1.60 ± 0.50	− 2.5	− 0.08
Fe	4000	69,000 ± 2100	67,000 ± 1700	2.9	1.18
Ga	1.31	22.6 ± 1.1	23.7 ± 5.1	− 4.6	− 0.22
[a]Sc	1.0	17.3 ± 1.1	17.3 ± 1.1	0.0	0.00
Co	1.1	19.0 ± 1.2	19.8 ± 1.5	− 4.0	− 0.53
Th	0.88	15.2 ± 0.8	14 ± 1	8.6	1.20

[a] Certified value

Table 4 Elemental concentrations in jarosite samples obtained using k_0 based IM-NAA method

Element	Energy (keV)	Sample-1		Sample-2	
		Relative conc. wrt Sc	Absolute concentration[a] (μg/g)	Relative conc. wrt Sc	Absolute concentration[a] (μg/g)
La	815.7	1.76	7.74 ± 0.32	2.58	6.97 ± 0.24
Na	1368.6	4920	22,000 ± 1500	3700	10,000 ± 900
As	559.08	228	1020 ± 50	267	720 ± 30
Sc	889.3	1	4.40 ± 0.11	1	2.70 ± 0.60
Fe	1099	58,000	255,000 ± 2300	54,000	146,000 ± 1100
Ga	834.08	44.8	197 ± 6	–	–
Zn	1115.5	6640	29,200 ± 100	17,600	47,500 ± 400
Ag	884	61.8	270 ± 10	71.9	194 ± 1
W	685.7	0.81	3.6 ± 0.1	5.89	16.0 ± 0.6
Au	411.8	0.037	0.20 ± 0.01	0.37	1.00 ± 0.08
Cd	527.9	16.6	73.0 ± 5.7	384	1040 ± 30
Cu	1345	835	3700 ± 130	–	–
Co	1173.2	–	–	5.08	13.7 ± 0.6
Sb	602	2.9	12.8 ± 0.5	84.7	230 ± 10

[a] Obtained using the absolute concentration of Sc which was determined by relative method

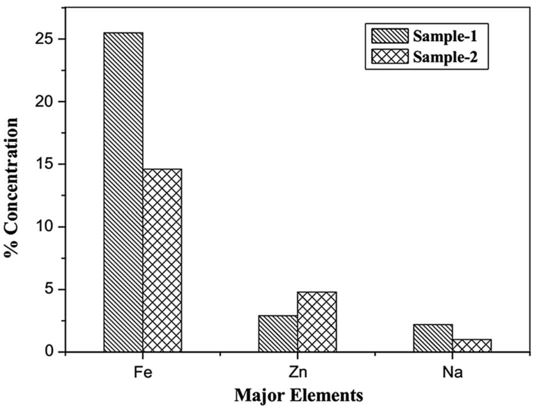

Fig. 8 Concentration (%) of major elements in jarosite samples

Conclusions

The dry tube positions of KAMINI reactor was characterized towards the development of k_0-based IM-NAA. The axial flux profile was obtained for the DT-1 and DT-2 and observed that the maximum neutron flux in DT-1 was (1.02 ± 0.02)E+10 cm^{-2} s^{-1} at 368 mm and (4.90 ± 0.30) E+7 cm^{-2} s^{-1} at 300 mm in DT-2, the position measured from its bottom. The f value for DT-1 at this location of maximum neutron-flux was found to be 144 ± 7 indicating the presence of more than 99% of thermal neutrons component. The α value of DT-1 was found to be -0.289 ± 0.010 indicating the existence of a hard epithermal neutron spectrum. The size of the DT-1 is sufficiently large and can therefore accommodate samples of varying sizes from mg to kg. An IAEA CRM SL-1 was analyzed by IM-NAA method in DT-1 and the elemental concentrations established using this method were found to be in good agreement with the certified values. The deviations were within ± 5% while the Z-score was found to be ± 1 for most of the elements. The jarosite samples were analyzed and the elemental profile consisting of 14 elements was reported. The elemental profile in jarosite samples obtained using IM-NAA indicates that these residues contain significant quantity of compounds of iron, zinc, cadmium, arsenic etc. The present DT-1 position of KAMINI reactor would be used in the future for the assay of irregular geometry samples in the fields of archaeological, forensic, nuclear, metallurgical etc. using k_0-based IM-NAA method. Similar study for the characterization of the other dry tube facility (DT-2) is in progress.

Acknowledgements We sincerely thank the reactor operational engineers of KAMINI reactor for their valuable support towards the irradiation experiments. We also thank health physicists and reactor physicists of IGCAR for their help for the radiation dose measurements of irradiated samples.

References

1. Bode P, Overwater RMW, De Goeij JJM (1997) Large-sample neutron activation analysis: present status and prospects. J Radioanal Nucl Chem 216:5–11
2. Overwater RMW, Bode P, de Goeij JJM, Hoogenboom JE (1996) Feasibility of elemental analysis of kilogram-size samples by instrumental neutron activation analysis. Anal Chem 68:341–348

3. Sueki K, Kobayashi K, Sato W, Nakahara H, Tomizawa T (1996) Nondestructive determination of major elements in a large sample by prompt γ ray neutron activation analysis. Anal Chem 68:2203–2209
4. Dasari KB, Acharya R, Swain KK, Lakshmana Das N, Reddy AVR (2010) Analysis of large and non-standard geometry samples of ancient potteries by internal monostandard neutron activation analysis using in situ detection efficiency. J Radioanal Nucl Chem 286:525–531
5. Acharya R, Nair AGC, Sudarshan K, Reddy AVR, Goswami A (2007) Development and applications of the k_0-based internal mono standard INAA method. Appl Radiat Isot 65:164–169
6. Nair AGC, Acharya R, Sudarshan K, Gangotra S, Reddy AVR, Manohar SB et al (2003) Development of an internal monostandard instrumental neutron activation analysis method based on in situ detection efficiency for analysis of large and nonstandard geometry samples. Anal Chem 75:4868–4874
7. Acharya R, Nair AGC, Reddy AVR, Goswami A (2004) Application of k_0-based internal mono standard instrumental neutron activation analysis method method for composition analysis of stainless steel clad sample. Anal Chim Acta 522:127–132
8. Greenberg RR, Bode P, Fernandes EADN (2011) Neutron activation analysis: a primary method of measurement. Spectrochim Acta Part B 66:193–241
9. De Corte F (2001) The standardization of standardless NAA. J Radioanal Nucl Chem 248:13–20
10. De Corte F, Simonits A, De Wispelare A, Hoste J (1987) Accuracy and applicability of the k_0-standardization method. J Radioanal Nucl Chem 113:145–161
11. Acharya R, Chatt A (2003) Characterization of the Dalhousie University SLOWPOKE-2 reactor for k_0-NAA and application to medium-lived nuclides. J Radioanal Nucl Chem 257:525–529
12. De Corte F, Simonits A (2003) Recommended nuclear data for use in the k_0 standardization of neutron activation analysis. At Data Nucl Data Tables 85:47–67
13. Overwater RMW, Bode P, de Goeij JJM (1993) Gamma-ray spectroscopy of voluminous sources corrections for source geometry and self-attenuation. Nucl Instrum Methods Phys Res A 324:209–218
14. Acharya R, Nair AGC, Reddy AVR, Goswami A (2004) Standardless analysis of Zircaloy clad samples by an instrumental neutron activation method. J Nucl Mater 326:80–85
15. Sudarshan K, Nair AGC, Goswami A (2003) A proposed k_0 based methodology for neutron activation analysis of samples of non-standard geometry. J Radioanal Nucl Chem 256:93–98
16. Kane WR, Mariscotti MA (1967) An empirical method for determining the relative efficiency of a Ge (Li) gamma-ray detector. Nucl Instrum Methods 56:189
17. Brahmaji Rao JS, Senthilvadivu E, Seshadreesan NP, Acharya R, Venkatasubramani CR, Reddy AVR (2012) Characterization of pneumatic fast transfer system irradiation position of KAMINI reactor for k_0-based NAA. J Radioanal Nucl Chem 294:137–141
18. Manh Dung Ho, Yeon Cho Seung (2003) A simple method for α determination. J Radioanal Nucl Chem 257:573–575
19. Manh Dung Ho, Fumio Sasajima (2003) Determination of α and f for k_0-NAA in irradiation sites with high thermalized neutrons. J Radioanal Nucl Chem 257:509–512
20. De Corte F, Moens L, Sordo-el Hammami K, Simonits A, Hoste J (1979) Modification and generalization of some methods to improve the accuracy of α-determination in the $1/E^{1+\alpha}$ epithermal neutron spectrum. J Radioanal Chem 52:305–317
21. De Corte F, Sordo-el Hammami K, Moens L, Simonits A, de Wispelare A, Hoste J (1981) The accuracy and precision of the experimental α-determination in the $1/E^{1+\alpha}$ epithermal reactor-neutron spectrum. J Radioanal Chem 62:209–255
22. De Corte F, Moens L, Simonits A, Sordo-El Hammami K, de Wispelaere A, Hoste J (1982) The effect of the epithermal neutron flux distribution on the accuracy of absolute and comparator standardization methods in (n, γ) activation analysis. J Radioanal Nucl Chem 72:275–286
23. Ashok Kumar GVS, Sen Sujoy, Radha E, Brahmaji Rao JS, Acharya R, Kumar R et al (2017) Studies on neutron spectrum characterization for the pneumatic fast transfer system (PFTS) of KAMINI reactor. Appl Radiat Isot 124:49–55
24. Mohapatra DK, Mohanakrishnan P (2002) Measurement and prediction of neutron spectra in the Kalpakkam mini reactor (KAMINI). Appl Radiat Isot 57:25–33
25. Mohapatra DK, Radha E, Mohanakrishnan P (2004) Theoretical and experimental investigations of reactor parameters in a U-233 fuelled research reactor. Ann Nucl Energy 31:197–212
26. Swain KK, Acharya R, Reddy AVR (2014) Analysis of SMELS by k_0-based IM-NAA method using PFTS position of KAMINI reactor for quality control exercise. J Radioanal Nucl Chem 300:33–37
27. https://www.hzlindia.com/bussiness/products-2/zink/. Accessed 20 June 2019
28. Pappu A, Saxena M, Asolekar SR (2006) Jarosite characteristics and its utilisation potentials. Sci Total Environ 359:232–243
29. Kerolli-Mustafa M, Ćurković L (2016) Analysing the characteristics and application potentials of jarosite waste in Kosovo. Glob NEST J 18:89–97